Int. J. Heat Mass Transfer. Vol. 23, pp. 373–385
Pergamon Press Ltd. 1980. Printed in Great Britain

SINGLE-PHASE AND TWO-PHASE MAGNETOHYDRODYNAMIC PIPE FLOW*

PATRICK F. DUNN
Engineering Division, Argonne National Laboratory,
Argonne, IL 60439, U.S.A.

(*Received* 11 *October* 1978 *and in revised form* 6 *August* 1979)

Abstract — Experimental results are presented for a range of measured temperatures and other parameters of vertically downward flows, both single-phase (sodium) and two-phase (sodium–nitrogen), in a conducting-wall pipe in the presence of a transverse magnetic field. Existing MHD theory predicted, to within experimental error, all single-phase pressure differences for magnetic interaction parameter values of up to approximately 100, beyond which the single-phase normalized resistance coefficients were noticeably lower than the laminar-flow predictions. The magnetic interaction parameter at which such deviation occurred was governed by the conductivity ratio. Two-phase pressure differences were obtained across a range of void fractions, approximately 0.3–0.8, where two distinct flow regimes were encountered. For those two regimes, the normalized resistance coefficients of pressure difference were predicted to within experimental error by the corresponding two-phase MHD pressure-difference models. In half of the two-phase cases examined, decreases were observed in normalized resistance coefficients at high values of the magnetic interaction parameter, a trend similar to that found in single-phase flow. The wall-voltage profiles of single-phase flows were symmetric with respect to the center of the applied magnetic field region; two-phase wall-voltage profiles were asymmetric because of the expansion of the gaseous nitrogen along the length of the test section. The influence of temperature and other system parameters upon pressure differences and wall voltages, and the possible effect of '*M*-shaped' velocity profiles in the two types of flow are discussed.

NOMENCLATURE

A, pipe cross-sectional area;
B, integral-averaged magnetic flux density;
d, internal pipe diameter;
K, average slip ratio, $u_{g,TP}/u_{l,TP}$;
l, electromagnet pole-face length;
$\dot{m}$, mass flow rate;
M, Hartmann number, $Bd\sqrt{\sigma_l/\mu_l}$;
N, magnetic interaction parameter, M^2/Re;
p, pressure;
Q, volumetric flow rate;
R_c, contact resistance;
R_{int}, internal flow resistance, equation (19);
R_{ext}, external flow resistance, equation (20);
Re, Reynolds number, $\rho_l u_l d/\mu_l$;
T, temperature;
u_l, average liquid velocity (single-phase), Q_l/A;
$u_{g,TP}$, average gas velocity (two-phase), $Q_g/\alpha A$;
$u_{l,TP}$, average liquid velocity (two-phase), $(Q_l/(1-\alpha)A)$;
u^s, superficial velocity, Q/A;
w, pipe wall thickness.

Greek characters

α, average void fraction;
δ, liquid–metal layer thickness;
Δp, pressure difference between transducers;
Δp^*, normalized pressure difference, $\Delta p_M - \Delta p_{M=0}$;
λ, resistance coefficient, $(-\Delta p/l)(2d/\rho u_l^2)$;
λ^*, normalized resistance coefficient, $\lambda_M - \lambda_{M=0}$;
μ, absolute viscosity;
ρ, density;
σ, electrical conductivity;
ϕ', conductivity ratio, $2w(\sigma_w + 1/R_c)/\sigma_l d$;
χ, mixture quality, $\dot{m}_g/(\dot{m}_g + \dot{m}_l)$.

Subscripts

l, liquid (sodium);
g, gas (nitrogen);
w, wall;
A, Region A;
B, Region B;
TP, two phase.

Acronyms

ANL, Argonne National Laboratory;
LMMHD, Liquid Metal; Magnetohydrodynamic;
OHD, Ordinary Hydrodynamic.

*This research was supported jointly by the Office of Naval Research and the U.S. Department of Energy.

INTRODUCTION

THIS study concerns the influence of a transverse magnetic field on the pressure difference and wall voltage in both single-phase (liquid metal) and two-phase (liquid metal-inert gas) vertically downward flows at various temperatures through a circular duct with conducting walls.

The primary motivation for this research is to develop a reliable method of predicting the total

pressure difference through two-phase liquid-metal magnetohydrodynamic (LMMHD) power generators under development at Argonne National Laboratory (ANL). Although many theoretical and experimental studies of single-phase MHD have been made for a variety of duct geometries and magnetic field alignments (for example, see comprehensive reviews by Hoffman and Carlson [1]; Hunt and Moreau [2]; Lielausis [3]; Reed [4]; Patrick [5]; Reed and Lykoudis [6]; Branover [7]) little consideration has been given to identifying the influence of a magnetic field (and, possibly, temperature and/or wall conductivity also) on two-phase liquid metal-gas flows. Two-phase LMMHD experiments with rectangular generator geometries have been conducted for a number of years at ANL [8–15]; in these, the pressure gradient has been measured as a function of line-averaged void fraction, magnetic flux density, and generator load factor. Relatively little work, however, has been directed toward relating local flow structure and properties to these overall measurements. Michiyoshi *et al.* [16] have reported experimental local void fraction profiles, bubble impaction rates, bubble velocities and their spectra measured for vertical upward mercury-argon, two-phase MHD pipe flow. Recent reports by Saito *et al.* [17, 18] have discussed redistributions of the gaseous phase in two-phase NaK–nitrogen flows subject to strong magnetic fields. The results of initial experiments in which hot-film and resistivity probes were used to measure local void-fraction and void-frequency profiles in a NaK–nitrogen LMMHD generator were presented recently by Fabris *et al.* [19]. An analytical model has been developed by Owen *et al.* [20] which is applicable to two-phase LMMHD generator channel flow at high Hartmann numbers.

Another motivation for this research lies in the need for proper design of the cooling blanket required in the proposed controlled thermonuclear reactors. Present designs [21] involve the pumping of a liquid metal through regions of high magnetic flux densities — possibly as high as 10 T — where the magnetic interaction parameter, the ratio of electromagnetic to inertial forces, is of the order of 10^4. The flow in this case is 'laminarized'; however, laminar-theory prediction of the flow's pressure gradient may not be adequate. Actual pressure gradients may be lower than the laminar-theory prediction when the magnetic interaction parameter value is high ($\gtrsim 100$), as reported initially by Pierson *et al.* [22] and indirectly supported by other experimental works [4, 16, 23].

The main objectives of this study, then, were to measure pressure differences and wall voltages over a range of flow velocities, void fractions, magnetic flux densities, and temperatures for a simplified test geometry; to identify possible alterations in both single-phase and two-phase pressure differences at high magnetic interaction parameter values; and to develop a means of correlating the pressure difference with other system parameters.

EXPERIMENTS

The present experiments were conducted at the ANL two-phase sodium–nitrogen LMMHD facility (Fig. 1). The facility provides prescribed flows of liquid sodium [design flow rate of 26 kg s^{-1} at 0.79 MPa absolute (115 psia) at 811 K] and gaseous nitrogen [design flow rate of 0.18 kg s^{-1} at 1.03 MPa absolute (150 psia) at 811 K] at temperatures from ~ 480 to 810 K (~ 400 to 1000°F). The sodium and nitrogen are mixed, passed through the test section duct in the presence of magnetic flux densities of up to 0.9 T, and then separated. The sodium is recirculated, and the nitrogen is vented to the atmosphere after removal of any traces of sodium carryover.

The sodium-loop components are an electromagnetic pump with blower, electromagnetic flowmeter, heat exchanger with blower, dump tank, piping and piping components, and valves. The nitrogen-loop components include a trailer of compressed nitrogen gas, flowmeter, heater, flow-rate controller, piping and piping components, and valves. The section of the loop through which the two-phase mixture circulates is the test-section duct and dump tank with primary and secondary separators. A d.c. iron-core electromagnet produces the magnetic field.

In these experiments a circular pipe 'mixer-generator' test section (Fig. 2) was employed in lieu of the actual mixer-LMMHD generator test section. Tests utilizing the 4 in. (~ 10 cm) dia., circular stainless steel pipe test section were conducted over a range of liquid mean flow velocities (2.0–4.2 m s^{-1}), mixture qualities (0–0.0053), magnetic flux densities (0–0.9 T), and temperatures (530–810 K).

The test section, 92.5 in. (~ 2.4 m) in length, contained a single orifice for gas injection (Fig. 2). The pressure difference along the test section was measured with two absolute-pressure transducers, located 102 in. (~ 2.6 m) apart, approximately at the entry and exit of the test section. Pressure measurements along the test-section length within the magnetic field region, like those performed by Reed [4], were not made. The inlet gas pressure was monitored with an additional absolute-pressure transducer, and inlet liquid and gas temperatures by means of thermocouples located between the outer pipe wall and the piping insulation. Mixture qualities were calculated from the sodium and nitrogen volumetric flow rates measured by electromagnetic and gas flowmeters respectively, inlet pressures and temperatures. A transverse magnetic field along 22.25 in (~ 0.57 m) of the approximate center region of the test section was provided by a d.c. iron-core electromagnet, the centerline flux density of which was determined by means of the voltage drop across the calibrated current shunt. Nineteen voltage probes, welded at 90° intervals about the circumference and at 6 in. (~ 0.15 m) intervals along the length of the test-section outer wall, both within and outside the pole-face region of the electromagnet, were utilized to monitor the wall voltages. All essential parameters were sequentially scanned and recorded during each

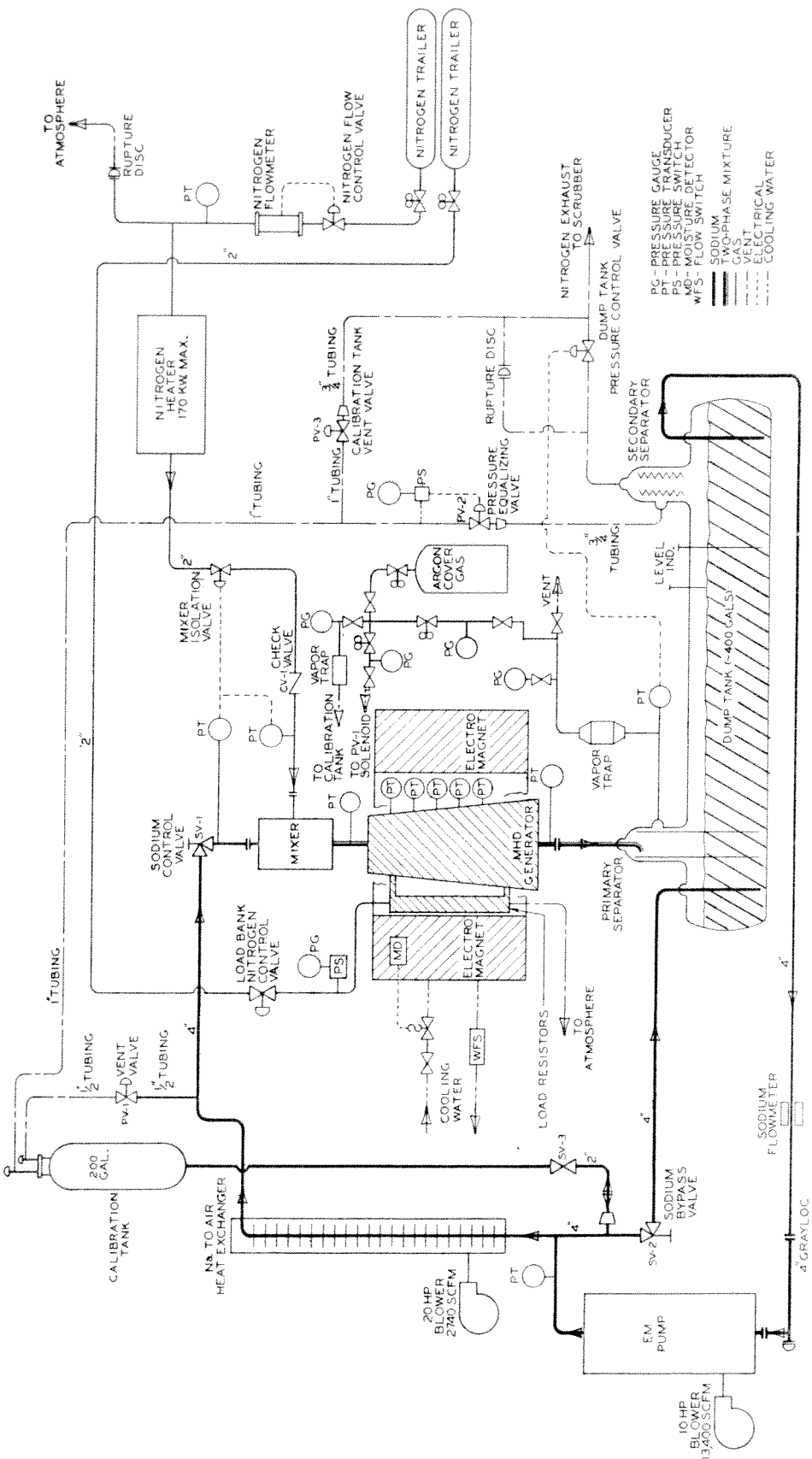

FIG. 1. Schematic of the sodium–nitrogen LMMHD facility.

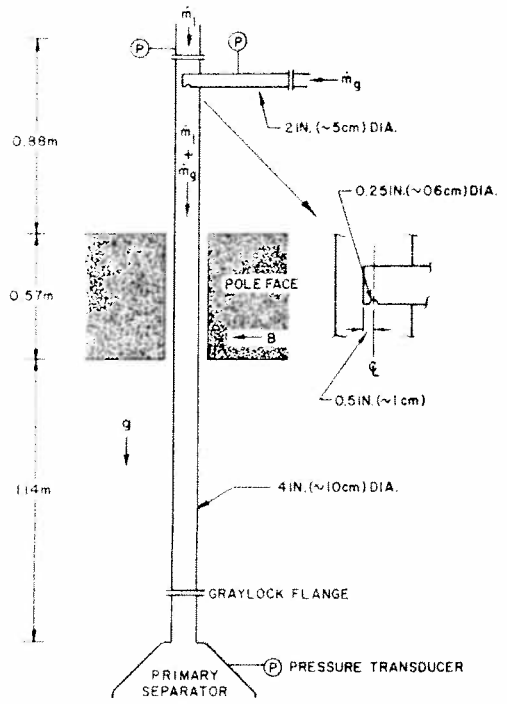

FIG. 2. Schematic of the circular-pipe test section.

experimental run by the data acquisition system of the facility. In addition to the sequential acquisition of data, the voltage differences between centerline 'positive' and 'negative electrode' voltage probes (numbers 12 and 5) and between two 'negative electrode' voltage probes (numbers 4 and 5) within the pole-face region were displayed, on both on an oscilloscope and a chart recorder.

Values of the standard estimates of error for the parameters measured were sodium mass flow rate, 3.1%, nitrogen mass flow rate, 5.1%, temperature, 0.5%, pressure, 3.5%, magnetic flux density, 0.6%, and wall voltage, 0.1%.

RESULTS

Single-phase pressure-difference results

All the single-phase pressure-difference data were expressed first in nondimensional form by their respective values of the single-phase resistance coefficient, λ. The MHD contribution to the pressure difference was then obtained by determining the corresponding single-phase normalized resistance coefficient, λ^*, for each single-phase Hartmann to Reynolds number ratio, M/Re, case examined, where

$$\lambda^* \equiv \lambda_M - \lambda_{M=0} = \left[\left(-\frac{\Delta p}{l}\right)\left(\frac{2d}{\rho_l u_l^2}\right)\right]_M - \left[\left(-\frac{\Delta p}{l}\right)\left(\frac{2d}{\rho_l u_l^2}\right)\right]_{M=0} \quad (1)$$

$$M \equiv Bd\sqrt{\sigma_l/\mu_l} \quad (2)$$

and

$$Re \equiv \rho_l u_l d/\mu_l. \quad (3)$$

In the above expressions d is the pipe internal diameter, u_l the average liquid velocity, and ρ_l, σ_l, and μ_l the sodium density, electrical conductivity, and absolute viscosity, in that order. B represents the integral-averaged magnetic flux density determined from the measured centerline flux density and the flux density profile. The pressure gradient for these cases was approximated by $\Delta p/l$, where Δp is the pressure difference between the transducers, and l the electromagnet pole-face length.

The single-phase Reynolds numbers ranged from 4.8×10^5 to 1.6×10^6; the single-phase Hartmann numbers ranged from 2.0×10^3 to 1.2×10^4, and in some cases were equal to zero. The Hartmann number in all cases not equal to zero was greater than that required to 'laminarize' the flow, according to the criterion for transition from turbulent to 'laminarized' flow set forth by Patrick [5].

The nondimensional representation of the single-phase pressure-difference data obtained at 620 K is shown in Fig. 3. All the single-phase pressure-difference data gathered over the 530 K to 810 K range are presented elsewhere [13]. For Hartmann-to-Reynolds numbers ratio values up to approximately 0.015, all the results obtained agreed within experimental error with the relation

$$\lambda^* = \frac{2M}{Re}\left(\frac{M\phi' + 1}{1 + \phi'}\right) \quad (4)$$

where the single-phase conductivity ratio, ϕ', a function solely of temperature, is defined as

$$\phi' \equiv 2w(\sigma_w + 1/R_c)/\sigma_l d \quad (5)$$

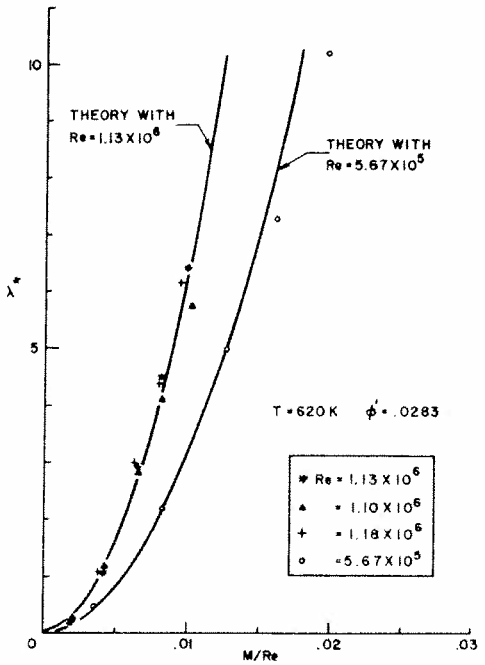

FIG. 3. Normalized resistance coefficient vs Hartmann-to-Reynolds numbers ratio for single-phase sodium flow $T = 620$ K.

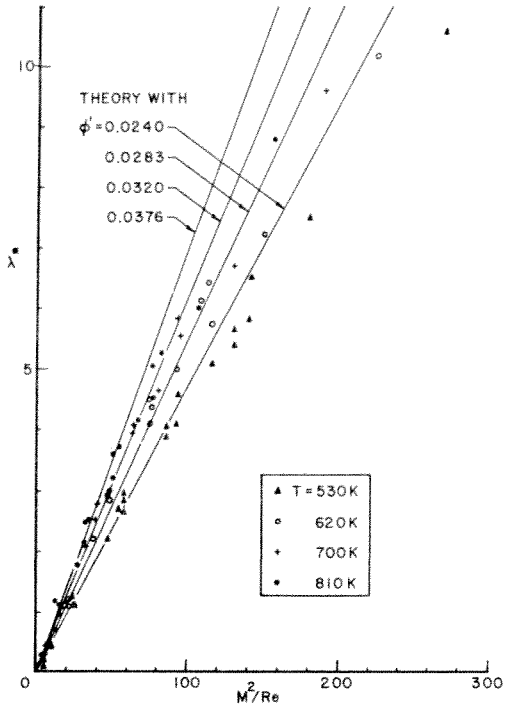

FIG. 4. Normalized resistance coefficient vs magnetic interaction parameter for single-phase sodium flow at various temperatures.

with w and σ_w representing the pipe wall thickness and electrical conductivity, and R_c the contact resistance between sodium and stainless steel [24]. Equation (4) represents the theory of Chang and Lundgren [25] developed for laminar MHD flow in a circular channel, with a conducting wall, in the presence of a magnetic field applied uniformly along its length. It does not consider magnetic field entrance and exit effects, as well as 'M-shaped' velocity profile effects, which were present in these experiments (see the Discussion section).

For most of the single-phase cases examined, values of the product $M\phi'$ were much greater than one. For these cases, (4) reduces to

$$\lambda^* = 2N\left(\frac{\phi'}{1+\phi'}\right) \tag{6}$$

where N represents the single-phase magnetic interaction parameter as defined by

$$N \equiv M^2/Re = \sigma_l B^2 d/\rho_l u_l. \tag{7}$$

The single-phase normalized resistance coefficients for all of the data obtained in the 530 K to 810 K range are plotted vs their respective single-phase magnetic interaction parameter values in Fig. 4. As shown in the figure, at magnetic interaction parameter values of approximately greater than 100, the measured values of the single-phase normalized resistance coefficients become lower than those predicted by (6). The magnetic interaction parameter value at which this departure occurred increased with decreasing conductivity ratio.

Two-phase pressure-difference results

In two-phase flow, the pressure gradient and void fraction, and thus the flow regime, are inherently coupled [26]. In these experiments, neither direct observation of the flow structure nor its inference from local diagnostic techniques were possible. The void

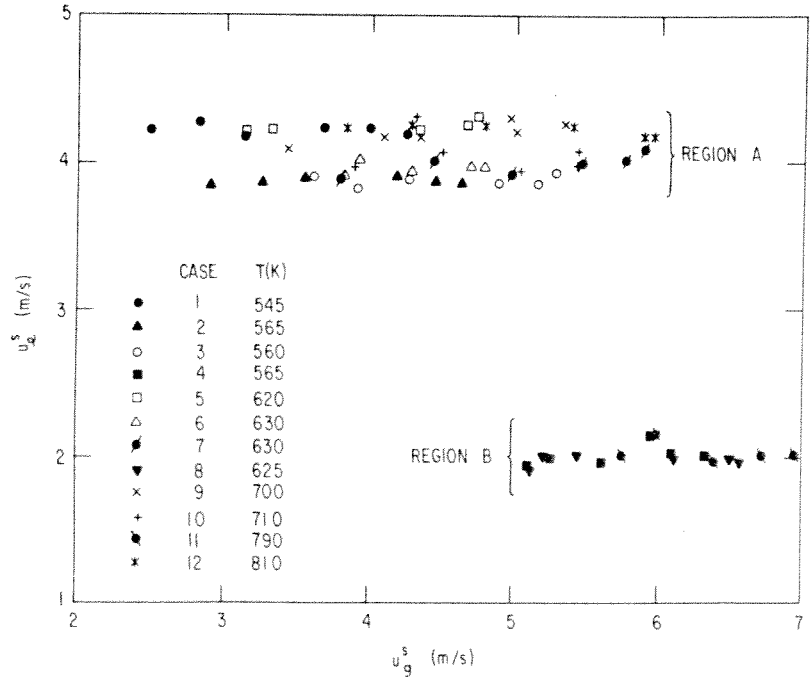

FIG. 5. Superficial liquid velocity vs superficial gas velocity for sodium–nitrogen flow at different temperatures.

fraction, also, was not measured and, hence, had to be determined in an indirect manner.

A wide range of void fractions were obtained in the present experiments by varying the liquid and gas flow rates over as large an operational range as possible [$13.9 \leq \dot{m}_l$ (kg s^{-1}) ≤ 31.0 and $0.054 \leq \dot{m}_g$ (kg s^{-1}) ≤ 0.077]. Possible flow regimes were delineated best by plotting superficial liquid velocity, u_l^s, against superficial gas velocity, u_g^s, as shown in Fig. 5. This method has been employed successfully by Taitel and Dukler [27] and many others [28] in studying ordinary hydrodynamic (OHD) liquid–gas flows, but it never has been used for MHD flow regime analysis. It can be seen readily that in these experiments two distinct groupings of data are present, denoted as Regions A and B in the figure. A majority of the data in Region A were obtained by operating the facility at high liquid and low gas flow rates. The data in Region B were obtained conversely.

For each of the cases examined, the average void fraction, α, at the horizontal pole-face centerline station along the axis of the flow was determined from the relation

$$\alpha = \dot{m}_g \rho_l / (\dot{m}_g \rho_l + K \dot{m}_l \rho_g) \tag{8}$$

in which $\dot{m}_l$ and $\dot{m}_g$ are the liquid sodium and gaseous nitrogen mass flow rates, ρ_l and ρ_g the liquid and gas densities, and K, the average slip ratio, equal to $u_{g,\,TP}/u_{l,\,TP}$. The density of the nitrogen, ρ_g, was determined from the pressure and temperature at the centerline station, where the pressure was found assuming that the measured pressure difference occurred solely within and varied linearly along the pole-face region. Values of the average slip ratio, K, were computed initially using the measured wall voltages and the expression for Ohm's Law applicable to this case, as described elsewhere in detail [15]. The resultant slip ratio values ranged from about 1.0 to 3.3. Since changes produced by the variation in K values from 1.0 to 3.3 in the two-phase normalized resistance coefficient were computed to be less than the standard estimate of the experimental error for this parameter, the mean value of K equal to 1.5 was chosen for all cases.

The void fraction range computed by this method for the data in Region A was from ~ 0.35 to ~ 0.70, and from ~ 0.70 to ~ 0.80 in Region B. The findings from OHD experiments similar in geometry and orientation to the present one [26] support that there are distinct flow regimes consonant with the void fraction ranges of these regions. Region A encompasses those flow regimes in which gas voids are dispersed throughout the cross-section of a liquid continuum, as depicted in Fig. 6. For Region A flows with lower average void fractions, the gas voids are predominantly various sized bubbles; whereas, for Region A flows with higher average void fractions, the gas voids are predominantly irregular shaped and sized slugs. Region B corresponds to an annular flow regime, as shown in Fig. 6. In this regime almost all the liquid is concentrated along the pipe wall, and the gas along the center of the flow.

Since the basic flow morphology of each region is distinctly different, it was necessary to develop a model for each region to predict the pressure difference.

(I) *Region A.* In Region A the two-phase mixture is considered to be homogeneous with respect to its density, viscosity, electrical conductivity and velocity. All these quantities are defined as functions of the average void fraction.

The rationale for this simplistic and approximate approach is that it has proven to be a very successful approach in modeling a variety of two-phase flow problems in the past [29], particularly in cases like the present, in which expressions for integral quantities are sought, such as the pressure difference over the length of a LMMHD generator. This type of approach was applied first by Thome [8] to model the pressure difference in two-phase LMMHD flows. Later, Tanatugu *et al.* [30] and Serizawa and Michiyoshi [31], and then Owen *et al.* [20] extended this approach to model two-phase LMMHD flows through both circular and rectangular geometries.

Following along these lines, the two-phase mixture's liquid velocity, electrical conductivity, density and viscosity are defined respectively as

$$u_{l,\,TP} = u_l/(1 - \alpha) \tag{9}$$

$$\sigma_{TP} \equiv \sigma_l \cdot \exp(-3.8\,\alpha) \tag{10}$$

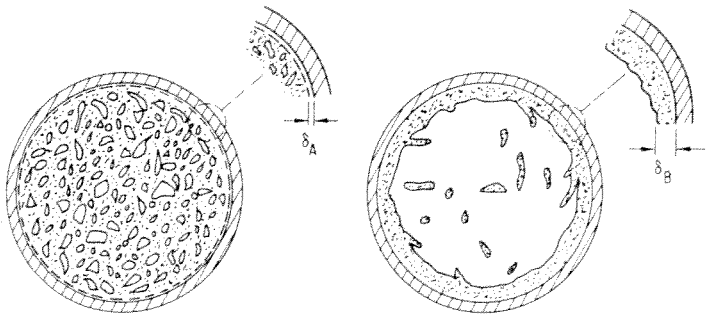

FIG. 6. Postulated two-phase flow morphologies for Regions A and B.

$$\rho_{TP} \equiv \rho_l \cdot f(\alpha) \tag{11}$$

and

$$\mu_{TP} \equiv \mu_l \cdot g(\alpha) \tag{12}$$

where α denotes the average void fraction, and $f(\alpha)$ and $g(\alpha)$ unprescribed functions of α. Expression (10) is the two-phase electrical conductivity model proposed by Petrick and Lee [32], which successfully has modeled the two-phase conductivity in LMMHD generators over the approximate void fraction range from 0.3 to 0.7. Expression (9) is derived purely from conservation of mass.

Expression for the two-phase equivalents of the Hartmann number, Reynolds number and conductivity ratio are developed using (2), (3), (5), and (9) through (12). They are

$$M_{TP} = M \cdot \sqrt{1/g(\alpha)} \cdot \exp(-1.9\alpha) \tag{13}$$

$$Re_{TP} = Re \cdot f(\alpha)/[(1-\alpha) \cdot g(\alpha)] \tag{14}$$

and

$$\phi'_{TP,A} = \phi' \cdot \exp(3.8\alpha). \tag{15}$$

The expression for the two-phase normalized resistance coefficient is

$$\lambda^*_{TP} = \left\{\left[\left(-\frac{\Delta p}{l}\right)\left(\frac{d}{2u_l^2}\right)\right]_M - \left[\left(-\frac{\Delta p}{l}\right)\left(\frac{d}{2u_l^2}\right)\right]_{M=0}\right\}\frac{(1-\alpha)^2}{f(\alpha)}. \tag{16}$$

The two-phase expression for Region A analogous to (4) becomes

$$\lambda^*_{TP,A} = \frac{2M}{Re}\,\frac{M\phi'\exp(1.9\alpha) + \sqrt{g(\alpha)}}{\phi'\exp(3.8\alpha) + 1} \cdot \frac{(1-\alpha)}{f(\alpha)} \cdot \exp(-1.9a). \tag{17}$$

This equation can be derived alternatively, as first suggested by Lykoudis [33], along the lines of Lockhart and Martinelli [34] by replacing the expression for the liquid-phase coefficient of friction in their theory with (4).

In all of the two-phase cases examined, values of the product $M\phi'\exp(1.9\alpha)$ were much greater than $\sqrt{g(\alpha)}$, where exact expressions for $g(\alpha)$ given by Wallis [26] and by Tanatugu *et al.* [30] were tested. Also, since $f(\alpha)$ is contained in both equations (16) and (17), the choice for its exact expression does not affect the difference between the experimental and theoretical values of the two-phase normalized resistance coefficient. With these considerations in mind, (17) reduces to

$$\lambda^*_{TP,A} = 2N\,\frac{\phi'}{\phi'\exp(3.8\alpha) + 1} \cdot (1-\alpha). \tag{18}$$

For simplicity of comparison, in (16) and (18) $f(\alpha)$ is assumed equal to one.

The two-phase normalized resistance coefficients of the measured pressure differences in Region A [computed using (16)] are compared with the two-phase MHD correlation given by (18) in Fig. 7. The linear least-squares fit of the data agreed well with the two-phase MHD correlation (correlation coefficient = 0.98, standard error of estimate = 0.31).

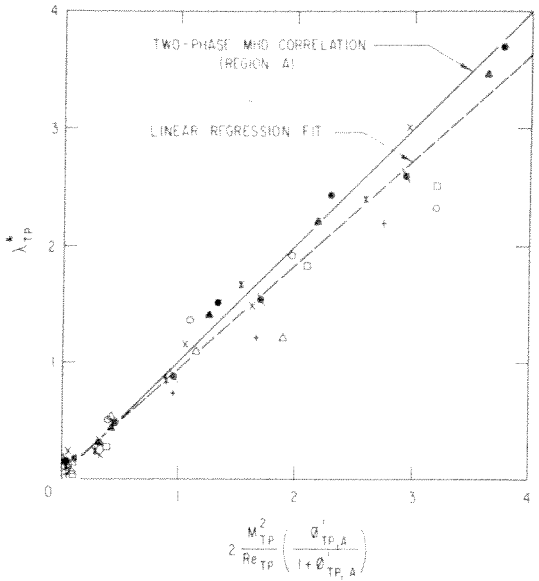

FIG. 7. Comparison of the two-phase MHD pressure-difference model with experimental results: Region A (symbol key same as in Fig. 5).

(II) *Region B.* In the present experiments, the pressure differences measured for Region B flows were found to be equal to approximately one-half the values of the pressure differences measured for Region A flows under similar MHD flow conditions. These reduced pressure differences, which are manifestations of the flow restructurization that occurs when present in Region B, can be predicted by a model developed for Region B. This model incorporates the flow morphology solely into the expression for the conductivity ratio and assumes that the two-phase equivalents of the Hartmann and Reynolds numbers derived for Region A flows remain unaltered, because they are expressed as functions of the average void fraction and are not strongly dependent upon the specific morphology of the flow.

As shown in Fig. 6, a typical flow cross-section for either Region A or B flows is comprised of a pure liquid–metal layer of thickness δ adjacent to the pipe wall, and a core flow of approximate diameter $d - 2\delta$, where d is the pipe internal diameter. The layer thickness and core conductivity, however, are different for each region. In both cases, the internal flow resistance, R_{int}, equals the resistance of the liquid–metal layer and core resistances in parallel, i.e.

$$R_{int} = d \Big/ \left\{2l\left[\delta\sigma_l + \left(\frac{d}{2} - \delta\right)\sigma_{TP}\right]\right\}, \tag{19}$$

where σ_{TP} represents the core conductivity. The external resistance is defined as

$$R_{ext} = d/[2lw(\sigma_w + 1/R_c)]. \quad (20)$$

Hence, the conductivity ratio applicable to both regions becomes

$$\phi'_{TP} \equiv R_{int}/R_{ext} = \frac{w(\sigma_w + 1/R_c)}{\delta\sigma_l + \left[\frac{d}{2} - \delta\right]\sigma_{TP}}. \quad (21)$$

For Region A flows, the liquid–metal layer resistance is much greater than the core resistance since δ is very small compared to $d/2$. Equation (21) then reduces to (15). For Region B flows, the core resistance becomes infinite since almost all of the liquid metal is concentrated in the liquid–metal layer adjacent to the pipe wall. Equation (21) then becomes

$$\phi'_{TP,B} = w(\sigma_w + 1/R_c)/\delta_B\sigma_l \quad (22)$$

where the subscript B denotes Region B.

The thickness δ_B can be found by noting that for annular flow the effective liquid-to-total flow cross-sectional area ratio approximately equals one minus the void fraction at that cross-section. One arrives at $\delta_B = d(1 - \sqrt{\alpha})/2$. Hence, (22) can be written as

$$\phi'_{TP,B} = 2w(\sigma_w + 1/R_c)/\sigma_l d(1 - \sqrt{\alpha}) = \frac{1}{1 - \sqrt{\alpha}}\,\phi' \quad (23)$$

where ϕ' is given by (5).

The two-phase expression for Region B analogous to (4) becomes

$$\lambda^*_{TP,B} = 2N\frac{\phi'}{\phi' + (1 - \sqrt{\alpha})}\cdot\frac{(1 - \alpha)}{f(\alpha)}\cdot\exp(-3.8\,\alpha) \quad (24)$$

since in all of the two-phase cases examined the product $M\phi'/(1 - \sqrt{\alpha})$ was much greater than one.

The two-phase normalized resistance coefficients of the measured pressure differences in Region B [computed using (16)] are compared with the two-phase MHD correlation given by (24) in Fig. 8. Here, for simplicity of comparison, $f(\alpha)$ is assumed equal to one. The linear least-squares fit of the data agreed well with the two-phase MHD correlation (correlation coefficient = 0.87, standard error of estimate = 0.37).

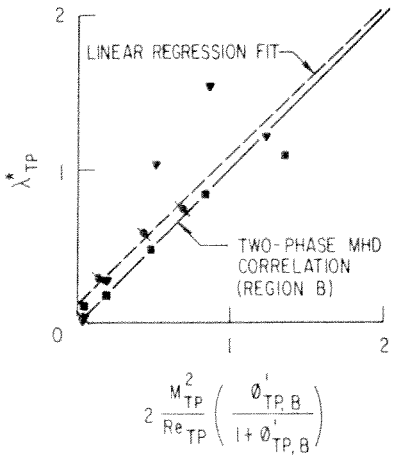

FIG. 8. Comparison of the two-phase MHD pressure difference model with experimental results: Region B (symbol key same as in Fig. 5).

Wall-voltage results

The wall-voltage profiles obtained for single-phase flow were symmetric with respect to the center of the applied magnetic field region and increased in magnitude with increasing magnetic flux density and flow velocity. Typical profiles obtained at 700 K and an average liquid velocity of 4.2 m s^{-1} are shown in Fig. 9, in which the probe locations with respect to the electromagnet pole-face horizontal centerline are indicated. At the highest flux density examined, 0.87 T, measurable voltages extended approximately 0.7 m upstream of the pole-face centerline. As expected for this compensated geometry, no noticeable shift in the magnetic field with fluid velocity was observed. All single-phase and two-phase wall-voltage data gathered over the 530 K to 810 K range are presented elsewhere [15].

The voltage profiles for two-phase flow were asymmetric about the pole-face horizontal centerline. Typical profiles obtained at 700 K and an average quality of approximately 0.00189 are shown in Fig. 10. In order to determine the cause of these asymmetries, the two-phase voltages measured along the test section length and inside the pole-face region were plotted against average liquid velocity, as displayed in Fig. 11. The linear fit for each magnetic flux density of wall voltage vs average liquid velocity demonstrated that the increase in the magnitude of the two-phase wall voltage within the pole-face region along the direction of flow was the result solely of the gas expansion along the flow.

DISCUSSION

In the present investigation several assumptions were made as a result of the sparsity of measurements within the magnetic field region of the test section. Pressure measurements within this region were not made. The MHD pressure gradient for fully established MHD flow within the region was approximated by the normalized pressure difference, calculated from pressures measured between two transducers located outside the magnetic field region, divided by the electromagnet pole-face length. This assumption is justifiable, provided magnetic field entrance and exit effects are not large.

It is difficult to assess the amount of error introduced by this assumption for cases of high magnetic interaction. The conditions under which magnetic-field entrance and exit effects are sufficient to alter the fully established MHD pressure gradient cannot be specified for the conducting-wall pipe configuration, since profiles of pressure along the direction of flow, measured before, within and beyond the magnetic field region have not been reported. The only complete pressure profile measurements for single-phase MHD

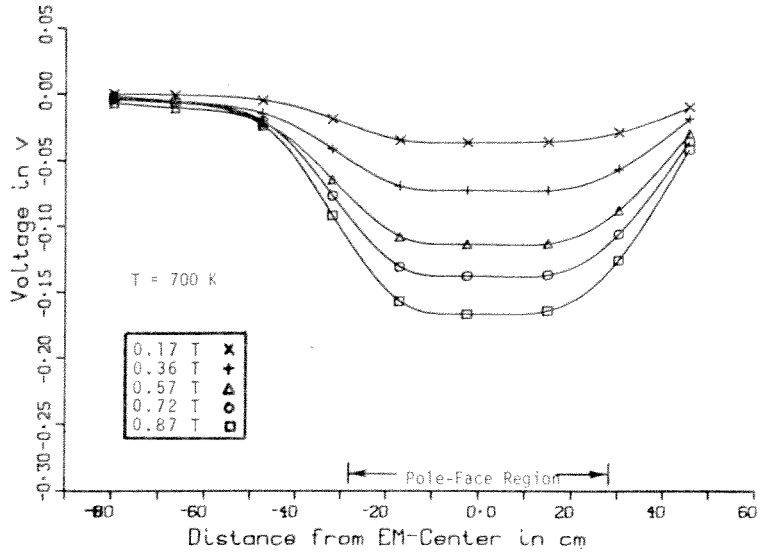

FIG. 9. Single-phase sodium wall-voltage distributions for various magnetic flux densities at $T = 700$ K.

flows presented in the literature are those of Fabris *et al.* [11], for the case of a rectangular LMMHD generator of expanding cross-sectional area. Branover [7] reported measurements which show magnetic-field entrance effects on the pressure gradient along the flow direction, for the case of an insulated-wall rectangular channel. Both these studies support that entrance and exit effects predominate only in cases of high magnetic interaction and mainly for insulated-wall configurations. In the light of this evidence and the excellent agreement between experimental and predicted normalized resistance coefficient values obtained in the present study, it appears that magnetic-field entrance and exit effects do not alter the fully established MHD pressure gradient in conducting-wall pipe flow up to magnetic interaction parameter values of approximately 100.

A corresponding estimate of the error in the two-phase case is not possible at present. For configurations in which the cross-sectional area of the test section along the direction of the flow is constant, a fully established two-phase MHD pressure gradient in the strict sense is never achieved. This is because the gaseous component of the mixture is continuously expanding, and the void fraction increasing, along the flow direction. Two-phase MHD measurements of this nature have not been reported.

As mentioned previously, the void fraction was not measured directly but was calculated from liquid and gas flow rates and densities assuming a constant value

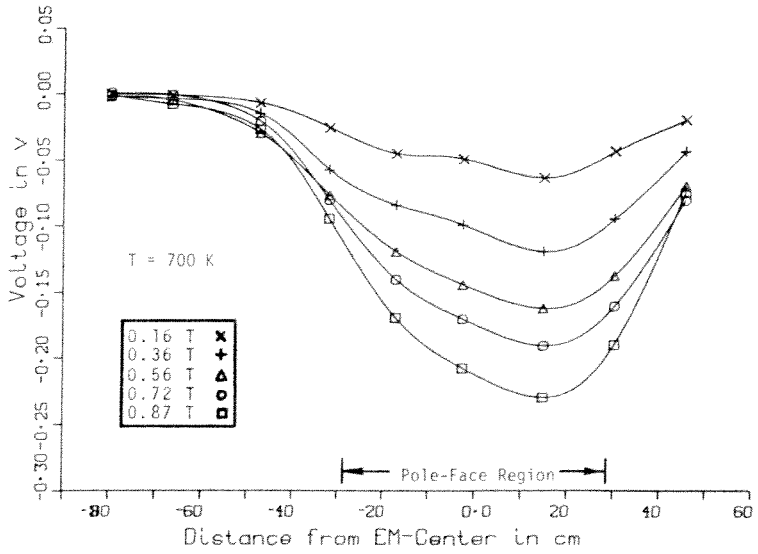

FIG. 10. Two-phase sodium–nitrogen wall-voltage distributions for various magnetic flux densities at $T = 700$ K.

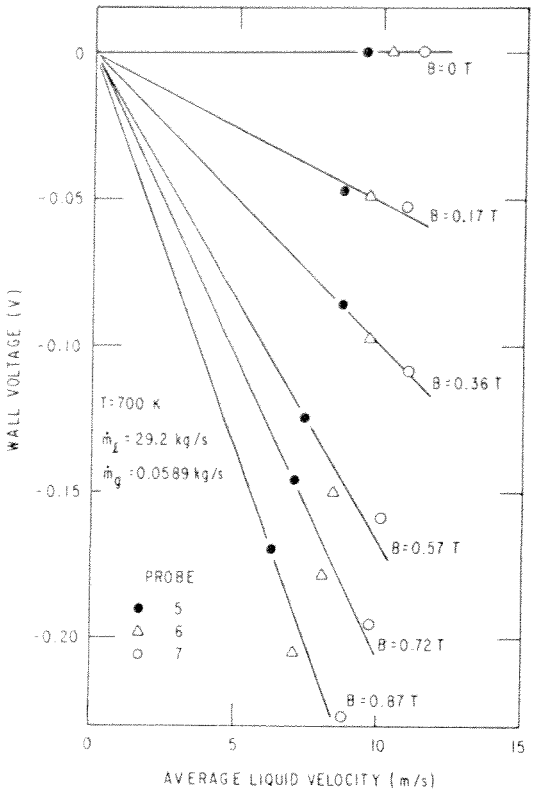

FIG. 11. Two-phase sodium–nitrogen wall-voltages vs average liquid velocity for voltage probes 5, 6, and 7 at various magnetic flux densities.

for the average slip ratio. This indirect determination of the void fraction leads to a standard estimate of error of 10%, assuming no error in the average slip ratio. There is, however, variance in slip ratio values under the present experimental conditions. The assumption of a constant slip ratio value for all cases introduces an additional error, resulting in a total standard estimate of error in the average void fraction of 27%. As a result of the magnitude of this error, the void fraction ranges of Regions A and B cannot be delineated precisely and should be considered approximate.

The theory of Chang and Lundgren predicted the single-phase normalized resistance coefficients of the measured pressure differences to within experimental error, provided that the contact resistance between sodium and stainless steel was considered and that the value of the magnetic interaction parameter was less than approximately 100. Under these conditions it appears that magnetic-field entrance and exit and '*M*-shaped' velocity profiles effects are small. Beyond magnetic interaction parameter values of 100, however, there is evidence that '*M*-shaped' velocity profiles were present.

The existence of '*M*-shaped' velocity profiles have been confirmed both experimentally and theoretically by Gnatyuk and Paramonova [23] for flow through a circular pipe with highly conducting walls. The mechanism of '*M*-shaped' velocity profile formation in a uniform flow with conducting walls is related to the presence of a current density gradient in the duct cross-sectional direction perpendicular to the applied magnetic field. Recently, Reed and Lykoudis [6] presented definitive experimental evidence for flow through a rectangular channel with insulated walls which linked decreases in the flow's resistance below laminar-theory predictions with the presence of '*M*-shaped' velocity profiles. Notwithstanding possible differences between these two cases in the mechanics of formation of these profiles, the signature of an '*M*-shaped' profile appears to be characteristically a decrease in the value of the resistance coefficient below its predicted value as the Hartmann-to-Reynolds number ratio is increased to a large value. These facts support that those decreases which were found to occur in the present investigation at values of the magnetic interaction parameter greater than approximately 100 most probably were the result of '*M*-shaped' velocity profiles. The magnitude of this decrease became accentuated with increasing Hartmann number or magnetic interaction parameter, and with increasing conductivity ratio.

There is also evidence that '*M*-shaped' velocity profiles were present in some the the two-phase cases examined. In six of the twelve two-phase cases, decreases with increasing magnetic flux densities in the slope of the two-phase normalized pressure difference versus magnetic flux density squared curve were measured. A typical case is shown in Fig. 12. The existence of '*M*-shaped' profiles have been verified indirectly in [16], which reported the presence of '*M*-shaped bubble velocity profiles in a circular tube, which were accentuated in magnitude with increasing flux density.

The two-phase MHD pressure-difference models developed for Regions A and B at present cannot be derived directly from the governing equations of continuity and momentum. Both these models employ the same two-phase equivalent Hartmann and Reynolds numbers expressions, and differ only in their

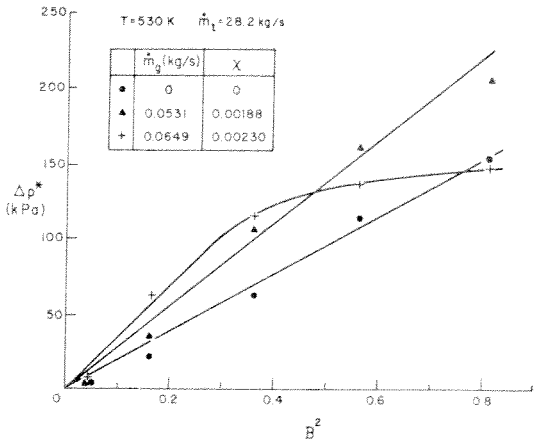

FIG. 12. Normalized pressure difference vs magnetic flux density squared for single-phase sodium and two-phase sodium–nitrogen at 530 K.

expressions for the two-phase conductivity ratio, which incorporates the morphology of the flow regime. Clearly, the two-phase normalized resistance coefficients predicted by these models are dependent upon the expressions chosen for the two-phase equivalents of the electrical conductivity, density and absolute viscosity. Under the present experimental conditions, the comparison between experimental and predicted values of the normalized resistance coefficient is affected only by the two-phase conductivity expression chosen, as shown previously. The two-phase conductivity expression employed in the present pressure-difference models was chosen because of its agreement with measurements in two-phase LMMHD generators over a wide void fraction range [12]. An alternative model could have been chosen. Yet, despite the simplicity of these models, both predicted quite successfully almost all of the data reported herein, and both encompass all of the parameters which govern these two-phase pressure differences.

In several of the two-phase cases examined it appears that transition from Regions A to B was brought about solely by an increase in magnetic flux density. Case 8 shown in Fig. 8 exemplifies such an instance, where at low magnetic flux densities the normalized resistance coefficient values are more consistent with those of Region A, but at a high magnetic flux density ($B = 0.87$ T) the value of the normalized resistance coefficient decreases noticeably. Similar transitions for the OHD case are accompanied by reduced pressure differences (Tong [35]). Such transition behavior has been noted to occur at times in ambient-temperature NaK–nitrogen LMMHD generators [9].

CONCLUSIONS

This study presented the results of pressure-difference and wall-voltage measurements for vertically downward flows, both single-phase and two-phase, in a conducting-wall pipe in the presence of a transverse magnetic field. It demonstrated that these pressure differences could be predicted to within experimental error, but that under certain conditions there were noticeable departures in measured pressure differences from predicted values. The nondimensional parameters which governed the occurrence of these departures were the Hartmann and Reynolds numbers, the conductivity ratio, and the average void fraction.

The measured single-phase pressure differences were predicted to within experimental error up to magnetic interaction parameter values of approximately 100, beyond which decreases from predicted values of the normalized resistance coefficient occurred. When the conductivity ratio was decreased, these departures occurred at higher magnetic interaction parameter values. These departures were interpreted to be the result of 'M-shaped' velocity profiles.

Two-phase pressure differences and wall voltages were measured over an approximate void fraction range from 0.3 to 0.8, where two distinct flow regimes were encountered. The normalized resistance coefficients of the pressure differences for both regimes were predicted to within experimental error by the corresponding two-phase MHD pressure-difference models, which had different expressions for the conductivity ratio. In half of the two-phase cases examined, decreases in normalized resistance coefficients at high values of the magnetic interaction parameter, similar in trend to those found in single-phase flow, were observed. For certain cases in which the average void fraction at low magnetic flux densities was just less than the critical void fraction for transition to annular flow, transition was brought about solely by an increase in magnetic flux density.

Acknowledgements — The author acknowledges Professor P. S. Lykoudis and Dr E. S. Pierson for their technical advice, Professor H. Branover for his discussions, Dr C. B. Reed and Dr B. F. Picologlou for their comments on this manuscript, and P. V. Dauzvardis and R. Vallrugo for their able assistance in conducting the experiments.

REFERENCES

1. M. A. Hoffman and G. A. Carlson, Calculation techniques for estimating the pressure losses for conducting fluid flows in magnetic fields. Lawrence Radiation Laboratory Report UCRL-31010 (1974).
2. J. C. R. Hunt and R. Moreau, Liquid–metal magnetohydrodynamics with strong magnetic fluids: a report on Euromech 70, *J. Fluid Mech.* **78,** 261–288 (1976).
3. O. Lielausis, Liquid–metal magnetohydrodynamics, *Atomic Energy Rev.* **13,** 527–581 (1975).
4. C. B. Reed, An investigation of shear turbulence in the presence of magnetic fields. Ph.D. Thesis, Purdue University (1976).
5. R. Patrick, Magneto fluid mechanic turbulence. Ph.D. Thesis, Purdue University (1976).
6. C. B. Reed and P. S. Lykoudis, The effect of a transverse magnetic field on shear turbulence, *J. Fluid Mech.* **89,** 147–171 (1978).
7. H. Branover, *Magnetohydrodynamic Flow in Ducts.* Wiley, New York (1978).
8. R. J. Thome, Effect of a transverse magnetic field on vertical two-phase flow through a rectangular channel. Argonne National Laboratory Report ANL-6854 (1964).
9. G. Fabris, R. L. Cole and R. G. Hantman, Fluid dynamic studies of two-phase liquid–metal flow in an MHD generator, *Proc. 6th Int. Conf. on MHD* **3,** 363–376 (1975).
10. G. Fabris, E. S. Pierson, A. K. Fischer and C. E. Johnson, Initial generator tests with revised ambient-temperature liquid–metal MHD facility, *16th Symp. Engng Aspects of MHD,* III.1.1–III.1.7, Pittsburgh, PA (1977).
11. G. Fabris, E. S. Pierson, I. Pollack, P. Dauzvardis and W. Ellis, High-power-density liquid–metal MHD generator results, *18th Symp. Engng Aspects of MHD,* D-2.2.1–D-2.2.6, Butte, MT (1979).
12. M. Petrick, Two-phase flow liquid metal MHD generator, *MHD Flows and Turbulence* pp. 125–245. Wiley (1976).
13. P. F. Dunn, G. Fabris, E. S. Pierson and M. Petrick, Two-phase liquid–metal MHD generator experiments and pressure–gradient correlations. *2nd Conference on MHD-Flows and Turbulence,* Bat-Sheva, Israel (1978).
14. P. F. Dunn, E. S. Pierson, J. D. Staffon, P. V. Dauzvardis and I. Pollack, High-temperature liquid–metal MHD generator experiments. *18th Symp. Engng Aspects of MHD,* D-2.2.7–D-2.2.12, Butte, MT (1979).

15. M. Petrick, P. F. Dunn, E. S. Pierson, P. V. Dauzvardis and I. Pollack, Liquid–metal MHD energy conversion, March 1976 to September 1977 Status Report, Argonne National Laboratory Report ANL/MHD-78-5 (1978).
16. I. Michiyoshi, H. Fanakawa, C. Kuramoto, Y. Akita and O. Takahashi, Local properties of vertical mercury–argon two-phase flow in a circular tube under transverse magnetic field, *Int. J. Multiphase Flow* **3**, 445–457 (1977).
17. M. Saito, S. Inoue and Y. Fujii-e, Gas–liquid slip ratio and MHD pressure drop in two-phase liquid metal flow in strong magnetic field. *J. Nucl. Sci. Technol.* **15**, 476–489 (1978).
18. M. Saito, H. Nagae, S. Inoue and Y. Fujii-e, Redistribution of gaseous phase of liquid metal two-phase flow in a strong magnetic field, *J. Nucl. Sci. Technol.* **15**, 729–735 (1978).
19. G. Fabris, P. F. Dunn, J. Z. Gawor and E. S. Pierson, Local measurements in two-phase liquid–metal MHD, *2nd Conference on MHD-Flows and Turbulence*, Bat-Sheva, Israel (1978).
20. R. G. Owen, J. C. R. Hunt and J. G. Collier, Magnetohydrodynamic pressure drop induced two-phase flow, *Int. J. Multiphase Flow* **3**, 23–33 (1976).
21. W. M. Wells, ORNL fusion power demonstration plant: lithium as a blanket coolant. Oak Ridge National Laboratory Report ORNL/TM-6214 (1978).
22. E. S. Pierson, P. V. Dauzvardis and P. F. Dunn, Sodium–nitrogen liquid–metal MHD facility initial test results, *16th Symp. Engng Aspects of MHD*, III.2.8–III.2.13, Pittsburgh, PA (1977).
23. V. V. Gnatyuk and T. A. Paramonova, Effect of the conductivity of the walls on the velocity profile in a circular tube, *Magnitnaya Gidrodinamika*, No. 1 (Eng. Trans.) 126–128 (1971).
24. L. B. Vandenburg, Electrical contact resistance between sodium and stainless steel. Knolls Atomic Power Laboratory Report KAPL-1502 (1956).
25. C. C. Chang and T. S. Lundgren, Duct flow in magnetohydrodynamics, *ZAMP* **12**, 100–114 (1961).
26. G. B. Wallis, *One-Dimensional Two-Phase Flow*. McGraw-Hill, New York (1969).
27. Y. Taitel and A. E. Dukler, A model for predicting flow regime transitions in horizontal and near horizontal gas–liquid flow, *A.I.Ch.E. J.* **22**, 47–55 (1976).
28. G. W. Govier and K. Aziz, *The Flow of Complex Mixtures in Pipe*. Van Nostrand Reinhold, New York (1972).
29. M. Ishii, One-dimensional drift-flux model and constitutive equations for relative motions between phases in various two-phase flow regimes, Argonne National Laboratory Report ANL-77-47 (1977).
30. N. Tanatugu, Y. Fujii-e and T. Suita, Frictional pressure drop for NaK–N_2 two-phase flow in a rectangular cross-section channel of large aspect ratio, *J. Nucl. Sci. Technol.* **10**, 219–226 (1973).
31. A. Serizawa and I. Michiyoshi, Void fraction and pressure drop in liquid–metal two-phase flow, *J. Nucl. Sci. Technol.* **10**, 435–445 (1973).
32. M. Petrick and K. Y. Lee, Performance characteristics of a liquid metal MHD generator, *Proc. Symp. on MHD Elec. Power Gen.* **2**, 953–970 (1964).
33. P. S. Lykoudis, Correlating performance data of two-phase liquid–metal MHD generators. Argonne National Laboratory LMMHD Group Memo 77-1 (1977).
34. R. W. Lockhart and R. G. Martinelli, Proposed correlation of data for isothermal two-phase, two component flow in pipes, *Chem. Engng Prog.* **45**, 39–48 (1949).
35. L. S. Tong, *Boiling Heat Transfer and Two-Phase Flow*. Wiley, New York (1967).

MAGNETOHYDRODYNAMIQUE A UNE OU DEUX PHASES POUR UN ECOULEMENT DANS UN TUYAU

Résumé — On présente des résultats expérimentaux pour des écoulements verticaux descendants, à une phase (sodium) ou deux phases (sodium–azote), dans un tuyau à paroi conductrice, en présence d'un champ magnétique transversal. La théorie MHD prédit, aux erreurs expérimentales près, les différences de pression pour une seule phase jusqu'à des valeurs atteignant approximativement 100 du paramètre d'intéraction magnétique, alors qu'au delà elles sont notablement plus faibles que les prévisions de l'écoulement laminaire monophasique. Le paramètre d'intéraction magnétique pour lequel apparait cette déviation est gouverné par le rapport de conductivité. Les différences de pression en diphasique sont obtenues pour des fractions de vide entre 0,3 et 0,8, pour lesquelles deux régimes d'écoulement ont été observés. Pour ces deux régimes, les coefficients normalisés de résistance de pression différentielles, sont prédits par les modèles MHD correspondants. Dans la moitié des cas diphasiques étudiés, on observe un diminution de ces coefficients pour les valeurs élevées du paramètre d'intéraction magnétique, une tendance semblable à celle trouvée pour l'écoulement monophasique. Les profils de tension électrique des écoulements monophasiques sont symétriques par rapport au centre de la région du champ magnétique appliqué; pour les écoulements diphasiques, ces profils sont dissymétriques à cause de l'expansion de l'azote dans le sens de la longueur de la veine d'expérience. L'influence de la température et des autres paramètres du système sur les différences de pression et sur les tensions à la paroi est discutée, ainsi que l'effet de profils de vitesse en M dans les deux types d'écoulement.

Errata for

"Single-Phase and Two-Phase Magnetohydrodynamic Pipe Flow"

Equation (5) in the subject paper should be replaced by:

$$\phi' \equiv \frac{2\, w\, \sigma_w}{\sigma_\ell d} \Big/ \left(1 + \frac{4\, w\, \sigma_w}{d^2/R_c}\right) \qquad (5).$$

For the range of cases examined in the subject experiments, the denominator in new equation (5) equals unity. Thus, equation (5) for these cases becomes:

$$\phi' \equiv 2\, w\sigma_w/\sigma_\ell d$$

This change in equation (5) neither alters any subsequent expressions in the paper nor noticeably affects the "theory" curves in Figures 3 and 4.

EIN- UND ZWEIPHASIGE MAGNETOHYDRODYNAMISCHE ROHRSTRÖMUNG

Zusammenfassung—Es werden Meßwerte von Temperaturen und anderen Parametern einer vertikalen Abwärtsströmung mit sowohl einphasigen (Natrium) als auch zweiphasigen (Natrium–Stickstoff) Strömungen durch ein Rohr mit leitfähiger Wand unter dem Einfluß querorientierter Magnetfelder angegeben. Die bestehende MHD-Theorie ermöglicht, alle einphasigen Druckdifferenzen für magnetische Einflußparameter bis zu Werten von näherungsweise 100 innerhalb experimenteller Fehlergrenzen zu berechnen, außerhalb dieses Bereichs waren die einphasigen spezifischen Widerstandswerte merklich niedriger als die rechnerischen Werte für laminare Strömung. Der magnetische Einflußparameter, bei dem solche Abweichungen auftraten, wurde durch das Leitfähigkeitsverhältnis bestimmt. Zweiphasendruckdifferenzen wurden im Bereich von Gasvolumenanteilen bis zu näherungsweise 0,3–0,8 ermittelt, wo zwei ausgeprägte Strömungszustände auftraten. Für diese zwei Strömungszustände wurden die spezifischen Widerstandsbeiwerte für die Druckdifferenz innerhalb der Fehlergrenzen des Versuchs durch das zugehörige Druckdifferenzmodell für zweiphasige MHD-Strömung richtig vorausgesaft. Bei der Hälfte der untersuchten Zwei-Phasen-Fälle wurde ein Anstieg des spezifischen Widerstandskoeffizienten bei großen Werten des magnetischen Einflußparameters, ähnlich wie der Verlauf bei der Einphasenströmung gefunden. Das Wandspannungsprofil der Einphasenströmung war in Bezug auf das Zentrum des magnetischen Feldbereichs symmetrisch; Zweiphasen-Wandspannungsprofile waren wegen der Ausdehnung des gasförmigen Stickstoffs entlang der Teststrecke asymmetrisch. Der Einfluß der Temperatur und anderer Systemparameter auf die Druckdifferenz und die Wandspannungen, sowie der Einfluß von 'M-förmigen' Geschwindigkeitsprofilen in der Zweiphasenströmung werden besprochen.

ОДНОФАЗНОЕ И ДВУХФАЗНОЕ МАГНИТОГИДРОДИНАМИЧЕСКОЕ ТЕЧЕНИЕ В ТРУБЕ

Аннотация — Представлены результаты измерений температур и других параметров однофазных (натрий) и двухфазных (натрий-азот) потоков, стекающих вертикально вниз в трубе с электропроводными стенками при наличии поперечного магнитного поля. Существующая МГД теория позволяет определить (с точностью до экспериментальной ошибки) все разности давлений для однофазного потока при значениях параметра магнитного взаимодействия примерно до 100. Выше этого значения нормированные коэффициенты сопротивления для однофазного потока намного ниже коэффициентов, рассчитанных для ламинарного потока. Параметр магнитного взаимодействия, при котором получаются более низкие значения коэффициентов сопротивления, определялся отношением электропроводностей. Разности давлений для двухфазного потока были получены в диапазоне объёмных газосодержаний, примерно 0,3–0,8, в котором отчётливо наблюдалось два режима течения. Для этих режимов нормированные коэффициенты сопротивления в зависимости от перепада давления рассчитывались в пределах экспериментальной погрешности с помощью соответствующих двухфазных МГД моделей. В половине рассмотренных случаев двухфазного течения наблюдалось уменьшение значений нормированных коэффициентов сопротивления при больших значениях параметра магнитного взаимодействия аналогично тенденции, наблюдаемой при однофазном течении. Распределение электрического напряжения на стенке при однофазных течениях оказалось симметричным относительно центра области приложенного магнитного поля; распределение напряжения на стенке при двухфазных течениях были асимметричными из-за расширения газообразного азота вдоль экспериментального участка. Рассмотрено влияние температуры и других параметров системы на перепад давлений и распределение напряжения на стенке и возможное влияние «М-образных» профилей скорости на эти два типа течения.